Research Article **Open Access**

I. Mintourakis*, G. Panou, and D. Paradissis

Evaluation of ocean circulation models in the computation of the mean dynamic topography for geodetic applications. Case study in the Greek seas

DOI: https://doi.org/10.1515/jogs-2019-0015
Received April 14, 2019; accepted December 10, 2019

Abstract: Precise knowledge of the oceanic Mean Dynamic Topography (MDT) is crucial for a number of geodetic applications, such as vertical datum unification and marine geoid modelling. The lack of gravity surveys over many regions of the Greek seas and the incapacity of the space borne gradiometry/gravity missions to resolve the small and medium wavelengths of the geoid led to the investigation of the oceanographic approach for computing the MDT. We compute two new regional MDT surfaces after averaging, for given epochs, the periodic gridded solutions of the Dynamic Ocean Topography (DOT) provided by two ocean circulation models. These newly developed regional MDT surfaces are compared to three state-of-the-art models, which represent the oceanographic, the geodetic and the mixed oceanographic/geodetic approaches in the implementation of the MDT, respectively. Based on these comparisons, we discuss the differences between the three approaches for the case study area and we present some valuable findings regarding the computation of the regional MDT. Furthermore, in order to have an estimate of the precision of the oceanographic approach, we apply extensive evaluation tests on the ability of the two regional ocean circulation models to track the sea level variations by comparing their solutions to tide gauge records and satellite altimetry Sea Level Anomalies (SLA) data. The overall findings support the claim that, for the computation of the MDT surface due to the lack of geodetic data and to limitations of the Global Geopotential Models (GGMs) in the case study area, the oceanographic approach is preferable over the geodetic or the mixed oceanographic/geodetic approaches.

***Corresponding Author: I. Mintourakis:** School of Rural and Surveying Engineering, National Technical University of Athens, Zografou, 15780, Greece, E-mail: mintioan@survey.ntua.gr
G. Panou, D. Paradissis: School of Rural and Surveying Engineering, National Technical University of Athens, Zografou, 15780, Greece

Keywords: dynamic ocean topography, marine geoid, mean dynamic topography, ocean circulation models, satellite altimetry, vertical datum unification

1 Introduction

The Mean Dynamic Topography (MDT) can be described as the permanent, stationary component of the dynamic ocean topography which, in principle, can be described as the global mean geostrophic surface circulation of the ocean (Bingham et al., 2008). The knowledge of the MDT is crucial for both oceanographers (Wunsch, 1998), since it gives valuable information about the ocean's geostrophic surface currents, as well as for geodesists (Rummel, 2001), since it permits the unification of independent Local Vertical Datums (LVD), the reduction from the Mean Sea Surface (MSS) to the marine geoid and the computation of the satellite altimetry derived free air gravity anomalies over the sea. From the above oceanographic and geodetic concepts, two basic approaches in computing the MDT have been extensively presented (Bingham et al., 2008, Maximenco et al., 2009, Woodworth et al, 2012):

a) Oceanographers have determined the global ocean circulation by means of hydrographic measurements of temperature and salinity (in situ data) from ships [Pugh and Woodworth, 2014]. Today, the oceanographic MDT is determined from numerical ocean models, which employ a set of dynamical equations, which are fed by in situ data sets, meteorological wind and air pressure information, and hydrological information. These ocean models take into account various a-priori assumptions for oceanic and atmospheric properties (such as salinity, temperature, pressure, sea level, wind forcing etc.) and they usually assimilate in-situ observations of the above properties or observations of additional parameters (e.g. Sea Level Anomalies - SLA and/or Sea Surface Temperature - SST), in order to achieve a fine-tuning of the model. This may be termed the oceanographic approach to MDT computation.

b) The geodetic approach, wherein the MDT is derived using the ellipsoidal height of the mean sea surface (MSS), or mean sea level (MSL), minus the geoid height (Andersen et al., 2018). The MSS heights are obtained by grids of MSS models computed from the Sea Surface Heights (SSH) observations from multiple satellite altimetry missions, after being properly processed, adjusted, unified and referenced to a common epoch and a common datum. The geoid heights are provided either from a Global Geopotential Model (GGM) or from the gridded geoid heights of a regional, purely gravimetric geoid model.

Any of the two approaches has its own characteristic advantages and limitations. The oceanographic approach computes the solutions of a hydrodynamic model on a grid, which provides spatial uniformity and, in theory, it can compute the ocean circulation down to it's finer scales, provided that the bathymetry of the region is well known, the initial conditions of the model are accurate enough, there is a dense network of sensors that provide continuous oceanic observations for assimilation in the model and, finally, a computer with sufficient computational power is available. The geodetic approach takes advantage of the latest satellite gravity/gradiometry missions, such as the CHAllenging Minisatellite Payload, CHAMP (Reigber et al., 1999), the Gravity Recovery and Climate Experiment, GRACE (Tapley et al., 2004), andthe Gravity Field and Steady-State Ocean Circulation Explorer, GOCE (Drinkwater et al., 2003). These missions provided knowledge of the Earth's gravity field and of geoid heights with great accuracy in the medium and the long part of wavelengths, in a uniform way and with global coverage. Thus, these satellite-only GGM's are ideal for global solutions of the MDT and have led to significant improvements in the calculation of the ocean MDT at scales down to 125 km (Mulet et al., 2012). The later MSS models provide a satisfactory accuracy at scales down to 25-30 km, hence, for resolving the MDT up to these scales, there is a need to resolve the geoid heights up to these wavelengths. This requires the availability of accurate gravity observations, with adequate and uniform spatial coverage throughout the region of interest. Unfortunately, dense and accurate marine and airborne gravity surveys are available only for a few regions of our planet.

The case study in the present paper, described as the Greek seas (Fig. 1), is probably the more demanding part of Mediterranean Sea in terms of computing the MSS and the MDT. Specifically, as explained in detail in the related literature, we note that:

- the combined geoid models use an a priori MDT solution that makes questionable the independency of their results for MDT studies (Rio et al., 2014a).
- the Rossby radius is of the order of 10 km in Mediterranean Sea (Rio et al., 2014a).
- the basin geometry is characterized by narrow straits and numerous islands that induce a complex short scale circulation with sharp coastal gradients (Poulain et al., 2012).
- the mean surface geostrophic circulation presents a complex pattern of currents with speeds below 30 $cm{\cdot}s^{-1}$ (Poulain et al., 2012).
- there is a critical issue in geoid modelling as the availability of terrestrial and marine gravity is more limited in the eastern Mediterranean and North Africa than in northern Europe (Woodworth et al., 2015). For the case study area there are no marine and/or airborne gravity data available in the North Aegean (northern of the 37th parallel), while the accuracy of the heterogeneous and spatially irregular marine and airborne gravity data available for the rest of the area is not known.
- the satellite gravity missions (such as GOCE, CHAMP, GRACE and their combined gravity products), in the shortest wavelengths they can resolve (80–133 km), present an error in geoid determination that is greater than the MDT signal in the case study area (Bingham et al., 2014).

Taking into consideration the above, we decided to implement the oceanographic approach over the geodetic one for the computation of the MDT in the case study area and examine the performance of two regional ocean models.

This work is organised as follows: in Section 2, we present the hydrodynamic models used by: i) the Mediterranean Forecasting System (Simoncelli et al., 2014) and ii) the Hellenic Centre for Marine Research POSEIDON Forecasting System (Soukissian et al., 1999) and we use the provided solutions of the Dynamic Ocean Topography (DOT)[1] over given time intervals in order to compute the two oceanographic MDTs. In Section 3, we present three additional MDT models, one computed with a purely oceanographic approach, another computed with the use of the geodetic approach and the last one computed with a mixed oceanographic/geodetic approach. We evaluate all five models using the known characteristics of the regional ocean circulation. In Section 4, we evaluate the accuracy of the DOT solutions provided by the ocean forecasting systems by comparing them with other independent data,

1 The associated absolute dynamic ocean topography (referred to as DOT) is SSH minus the marine geoid. For given time intervals, DOT can be expressed as the average sea surface height relative to the marine geoid.

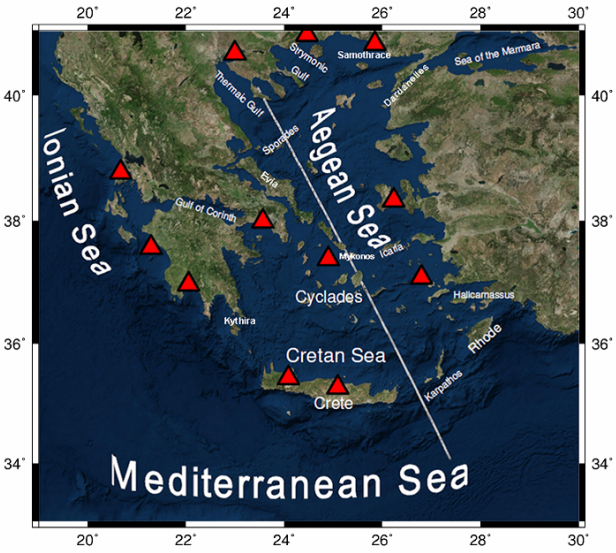

Fig. 1. The case study area described as the Greek seas with the names of the geographic features (islands, seas, gulfs, straits etc.) referred in the present study. The red triangles represent the positions of 12 tide gauge sites and the white line represents the Jason-2 satellite's footprint during its descending pass, track number 94, used for testing purposes (see Section 4).

such as tide gauge records of sea level and satellite altimetry along track SSH observations and SLA grids. Finally, in Section 5, we discuss the results of our study and make proposals for possible improvements for the MDT computation and research related to the LVD unification in our case study area.

2 Oceanographic approach to the Mean Dynamic Topography

In the first step, we obtain the DOT solutions provided over given time intervals by two different ocean circulation models. The one is used by the Mediterranean Forecasting System physical reanalysis (MFSpr) component (Simoncelli et al., 2014) and the other is used by the POSEIDON forecasting system developed and adapted for Aegean Sea (Nittis et al., 2006; Korres et al., 2002). By computing the mean of these DOT solutions for an extended period of time, we compute two new MDT models for the Greek seas. However, before presenting the used ocean circulation models, the computed MDTs and their evaluation, we need to clarify the issues related to the use of an oceanographic MDT for geodetic applications.

Dynamic heights of the sea surface computed by the hydrodynamic equations of an Ocean Model (OM) depend on a given value of gravity (g) used in the calculations. Different values of g (depending on the International Gravity Formula used by the OM) produce no noticeable difference in the sea surface dynamic height computed by the OM. Nevertheless, variations on the initial conditions adopted by an OM (such as the "climatology" values set for temperature and / or salinity T_{clim}, S_{clim}) correspond to a difference on the level of the zero-dynamic height of this OM. The values of these physical quantities (T_{clim}, S_{clim}, P_{atm}), along with the normal value of g adopted by the OM, are referred hereafter as the 'normal' values. These 'normal' values virtually define the OM's zero level for the dynamic heights that corresponds to the $z=0$ equipotential surface of the geoid with a value of gravity equal to g. After averaging, for a given epoch, the DOT solutions provided by an OM, we compute the MDT for this specific epoch. Comparing MDT surfaces computed by different OMs (referenced on the same epoch), one may notice an almost identical image of the MDT surface, with very similar surface gradients that correspond to similar patterns of ocean circulation. However, the mean difference of the MDTs might have a rather large value and this can relate to the fact that various OM's adopt different 'normal' values. In the oceanographic approach, the geoid heights are computed after subtracting the MDT values from the MSS heights. Thus, the concept of the 'normal' values of an OM has to be taken into account when computing a geoid with the oceanographic approach, as they define the zero height of the geoid. When computing the geoid with the oceanographic approach, it is also critical to adjust any difference between i) the 'normal' value of the atmospheric pressure P_{atm} (on the sea surface) used by the OM (for estimating the dynamic height of the sea surface), and ii) the reference value of the atmospheric pressure (on the sea surface) applied for the computation of the Inverse Barometric (IB) effect when computing the MSS from satellite altimetry data. Based on this concept, we define the values of the g, T_{clim}, S_{clim} and P_{atm} used by an OM to compute the MDT surface as the MDT's 'datum values'. Ideally, the MDT 'datum values' should be the same to the corresponding physical quantities adopted by the models of the MSS (P_{atm}) and of the geoid (g).

2.1 Short description of the ocean forecasting models

The first OM examined is part of the MFSpr component. It is an Ocean General Circulation Model (OGCM), with codes supplied by the Nucleus for European Modelling of the Ocean, NEMO (Madec et al., 1998) and a varia-

tional data assimilation scheme (OceanVAR) for temperature and salinity vertical profiles and satellite Sea Level Anomaly along track data. The model applies primitive equations in spherical coordinates and is implemented in the Mediterranean with a horizontal resolution of 1/16° and 72 unevenly spaced vertical levels (Oddo et al., 2009). The model extends into the Atlantic, in order to better resolve the exchanges with the Atlantic Ocean at the Strait of Gibraltar, while the Dardanelle straits inflow is also taken into account. The assimilated data include: sea level anomaly, sea surface temperature, in situ temperature profiles by VOS XBTs (Voluntary Observing Ship-eXpandable Bathythermograph), in situ temperature and salinity profiles by argo floats and in situ temperature and salinity profiles from CTD (Conductivity-Temperature-Depth). The model provides daily-mean and monthly-mean solutions of the Absolute Dynamic Topography (ADT) for the period from Jan 1^{st} 1987 to Dec 31^{st} 2016.

The second OM is part of the POSEIDON forecasting system for Aegean Sea and is based on the Princeton Ocean Model (POM) (Blumberg and Mellor, 1987). The model provides solutions of the ocean circulation on a regular grid, bounded between 19°E - 30°E and 30°N-41°N, with a resolution of 1/30° and it is developed on 24 σ-layers. Regarding the boundary conditions on the eastern and the western open edges, the model implements a coupling scheme (Korres and Lascaratos, 2003) with solutions provided by i) the Mediterranean Ocean Forecasting System model and ii) the hydrodynamic model for the Mediterranean used in the POSEIDON system. The model also takes into account the inflow of fresh water coming from the major Greek rivers, while the exchange through the Dardanelle straits is approximated on the concept of open boundary conditions. The circulation model uses, as a surface boundary condition for the ocean response to the atmospheric forcing, a high resolution (1/20°) atmospheric model included in the Poseidon forecasting system. The model assimilates observational data sets including AVISO sea level heights, AVHRR sea surface temperature, MEDARGO floats, temperature and salinity profiles and XBT data and provides high frequency solutions of the Free Sea Surface Height (FSSH) with a period of 6 hours (Korres et al., 2009).

Both the ADT and the FSSH are considered as DOT heights, which is the elevation of the SSH above the geoid. This is evident for ADT, as long as it is another definition of the DOT. On the other hand, the FSSH corresponds to a dynamic height described as the surface elevation η of the free sea surface with respect to a reference surface of zero height $z=0$. This reference surface of a constant dynamic height can be considered as an equipotential surface very close to or exactly at the surface of the geoid. Thus, the η quantity computed by the POM (the FSSH quantity computed by POSEIDON forecasting system) is considered as elevation of the sea surface above the geoid.

2.2 Computation of the new Mean Dynamic Topography surfaces

The DOT solutions of the MFSpr, given by its OGCM, were used to compute the MDT for an extended epoch covering a period of 20 years. To this effect, we downloaded the data of the daily mean DOT solutions from 1^{st} Jan. 1993 to 31^{st} Dec. 2012 and we computed the mean of each value for every cell of the grid. Thus, the so-called Mediterranean Forecasting System physical reanalysis Mean Dynamic Topography (MFSprMDT) was computed for the case study area (Fig. 2, top). In a similar manner, we downloaded the data of the non-assimilated solutions of the 6-hourly mean of the DOT, provided by the OM hosted in the POSEIDON forecasting system. Since the server of POSEIDON was out of service in the last year (and still is), we used only 4 years of data that were available, covering the period from 1^{st} Jan. 2008 to 31^{st} Dec. 2011. After computing the mean value of the 4-year DOT solutions for every cell of the grid, we created the so-called POSEIDON forecasting system non-assimilated Mean Dynamic Topography (POSnaMDT) for the area of the case study (Fig. 2, bottom).

For each one of the above MDT models, we applied the geostrophic equations and computed (a) the mean zonal, *U,* and (b) the mean meridional, *V,* vector components of the mean velocity of the ocean's surface currents. In this way, we draw the corresponding vectors and we examine the ocean surface circulation related to the MDT of each model for the case study area.

3 Comparisons with other Mean Dynamic Topography models

In order to evaluate further the two new regional MDT models, we compare them to three state-of-the-art models representing the oceanographic, the geodetic and the mixed type methodologies for the estimation of the MDT, respectively. These state-of-the-art models are i) the SMDTMed2014 (Synthetic Mean Dynamic Topography for the Mediterranean 2014, Rio et al., 2014a), ii) the MDTCNES-CLS13 (Mean Dynamic Topography, estimated by the Center National d'Etudes Spatials 2013, Rio et al., 2014b), and iii) the DTU10MDT (Danish Technical University 2010 Mean Dynamic Topography, Knudsen and Ander-

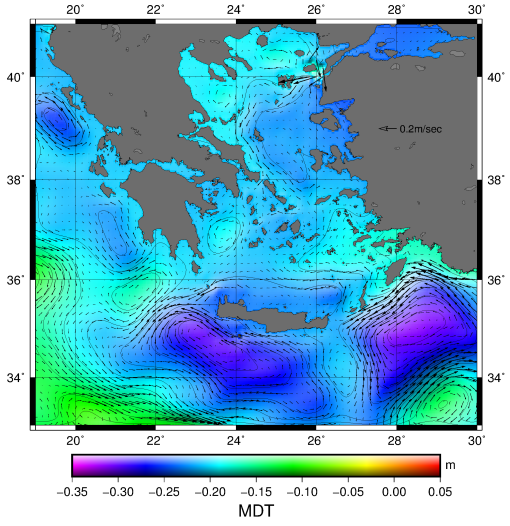

(a)

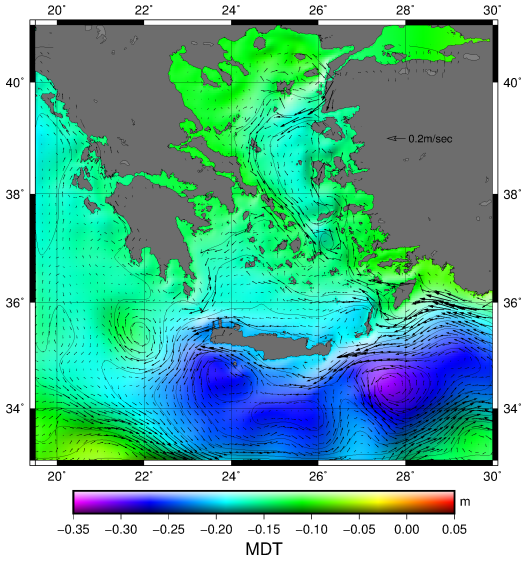

(b)

Fig. 2. (a) The MFSprMDT model for the area of the Greek seas. The vectors represent the ocean's surface currents calculated by the geostrophic equations. (b) The POSnaMDT model for the area of the Greek seas. The vectors represent the ocean's surface currents calculated by the geostrophic equations.

sen, 2013). For each model, we present the graphs and the statistics of the MDT surfaces and of their velocity vector fields. The comparisons are performed numerically, by using the SMDTMed2014 as a reference model, and qualitatively, by presenting and interpreting the ocean circulation characteristics that each model presents.

The general ocean circulation of the study area (determined by Karageorgis et al., 2008) is presented in Fig. 3, in order to serve as a comparison to the geostrophic circulation indicated by the above models. It should be noted that the occurrence of a geostrophic current perpendicular to a coastline, or the occurrence of a false strong current close to it, indicates an incorrect value of the MDT and, consequently, an error in the separation value between the MSS and the geoid surfaces along this coast. In addition, the velocity of the geostrophic currents is proportional to the slope gradient of the surface of the MDT and vice versa. This comparison is not quantitative (does not compare parameter values) but qualitative (recognises the existence or absence of known characteristics). Nevertheless, it is considered as critical, since the appearance of false characteristics or the inability to display well-known currents in the case study area designates a weakness to model correctly the regional MDT. Although this comparison is done with oceanographic criteria, it is not of oceanographic interest but has clear implications to geodetic applications that require the knowledge of the MDT.

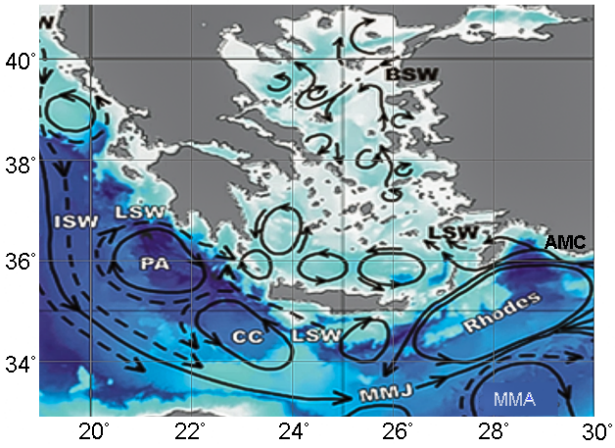

Fig. 3. The general ocean surface circulation with the major cyclonic and anti-cyclonic systems in the case study area (Karageorgis et al., 2008).

3.1.1 The MSprMDT model

In the geostrophic ocean surface circulation as calculated by the MSprMDT model (Fig. 4 and Tab. 1 & Tab. 2), the following systems are clearly evident: i) the strong Asia Minor Current (AMC), which passes south of the coasts of the Rhodes island, ii) the outflow of the Black Sea Water masses (BSW) through the Dardanelles straits and iii) the current of North Aegean Sea (NAC) between the Sporades islands and the eastern coasts of the island of Evia. The cyclone of Rhodes (RC) south-east of the island of Rhodes, the Cretan Cyclone (CC) south of the island of Crete, the Kerkyra Cyclone (KC), Myrtoan Sea Anti-cyclone (MA), the Pelopa Anti-cyclone (PA) south of the cape Tainaro and the Mersa-Matruh Anticyclone (MMA) in the south-eastern boundary of the case study area, are also evident. One can also notice an inflow of water masses in Cretan Sea basin through the straits between the islands of Rhodes, Karpathos and Crete and an outflow through the strait between the islands of Kythira and Crete. This inflow-outflow pattern presents the exchange of water masses between the basins of Mediterranean Sea and Cretan Sea.

3.1.2 The POSnaMDT model

In the case of using the POSnaMDT model (Fig. 5 and Tab. 1 & Tab. 2), the AMC is also clearly evident and it presents a strong jet around the Rhodes island and across the southern coasts of the island of Karpathos, up to the island of Crete. It is also observable that the outflow of the BSW runs through the Dardanelles strait, and that the NAC, after running between the Sporades islands across the eastern coasts of the island of Evia, crosses north of the Cyclades islands and flows towards South Aegean Sea through the strait between the islands of Icaria and Mykonos. The systems of the RC, the CC, the PA and the MMA are also evident, as in the case of the MSprMDT models. Finally, the same ocean surface circulation patterns, which denote the exchange of water masses between Mediterranean Sea and Cretan Sea basins, are also present.

Regarding the two new regional MDT models, we notice no significant differences between them, based on the statistics of their elevations (Table 1) and the images of their patterns of ocean surface currents and cyclonic/anti-cyclonic systems they predict (Figs. 4 & 5). A difference of 3.6 cm is noticed between the mean values of the two MDTs but we have to take into account that they refer to different epochs. For this reason we re-computed the MFSprMDT to the same epoch to the POSnaMDT epoch (2008 - 2011), and we found that the aforementioned difference turns out

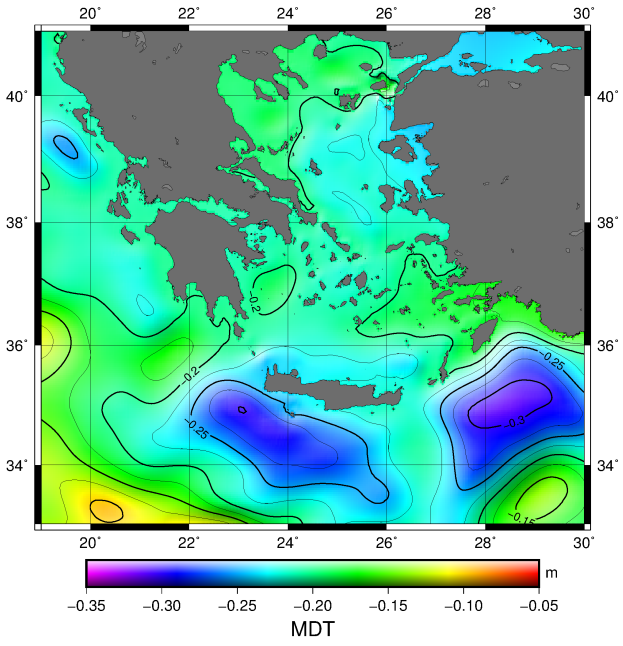

(a)

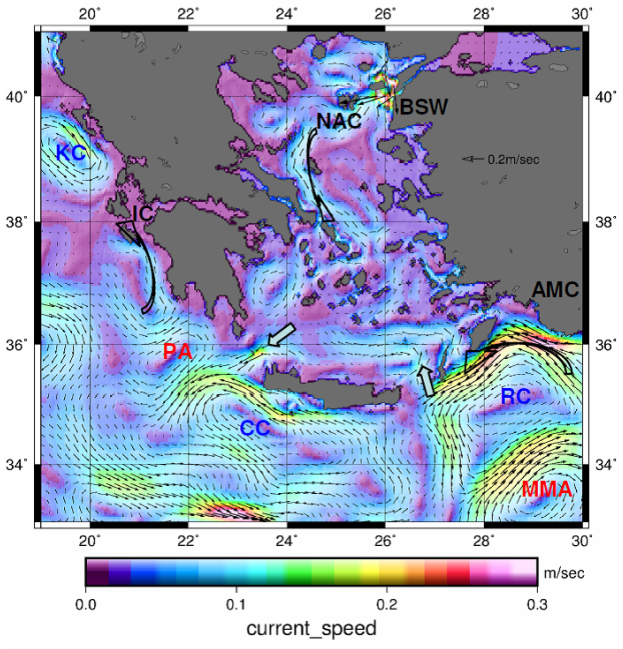

(b)

Fig. 4. (a) The heights of the MSprMDT model. (b) The geostrophic ocean surface circulation as calculated by the MSprMDT model.

smaller than 2.6 cm. Thus, the major part of the 3.6 cm difference cannot be attributed to the different epochs that each MDT is referenced to, but to the presented concept of the MDT 'datum values'. Furthermore, the MFSprMDT presents smaller statistics (Table 1) for the range and standard deviation of its elevations with respect to the corre-

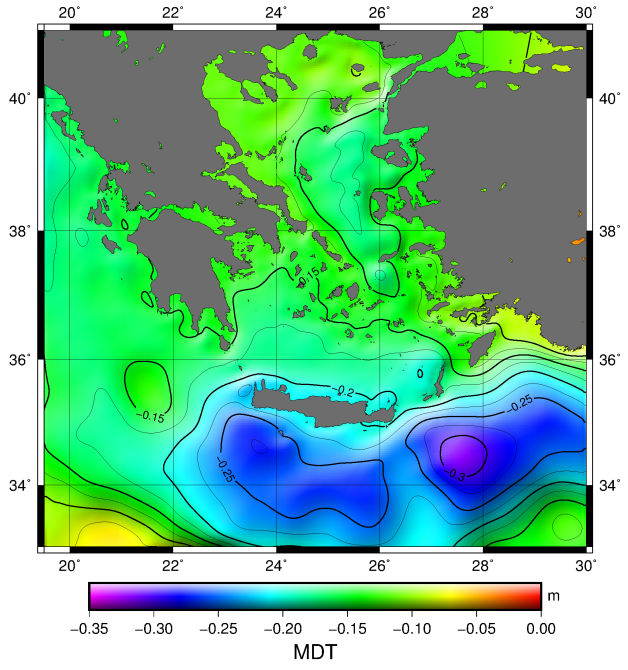

(a)

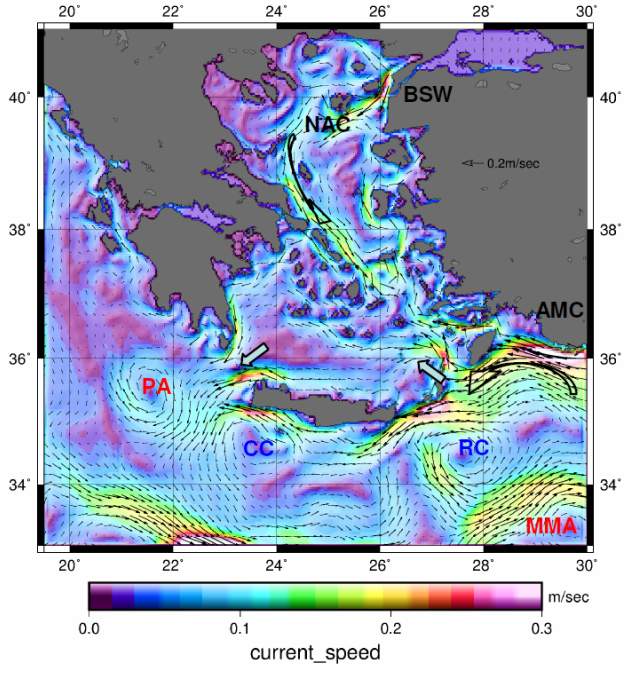

(b)

Fig. 5. (a) The heights of the POSnaMDT model. (b) The geostrophic ocean surface circulation as calculated by the POSnaMDT model.

sponding statistics of the POSnaMDT or the MFSprMDT (epoch 2008 - 2011). This is due to the big difference in the length of the averaging periods used in each case. Since averaging acts like a smoothing filter, it is expected that the 20 years period, used in the case of the MFSprMDT model, should present a stronger smoothing effect than the smoothing effect caused by the 4 years period used in the case of the POSnaMDT model.

3.1.3 The SMDTMed2014 model

The SMDTMed2014 model (Fig. 6 and Tab. 1 & Tab. 2) provides values of the MDT heights on an rectangular grid with a 1/16-degree resolution. This model also refers to the 1993-2012 epoch, the same as the MFSprMDT epoch, and its implementation follows a purely oceanographic methodology for the calculation of the MDT, using the results of an ocean circulation model, combined with satellite altimetry, derived SLA observations and in-situ oceanographic data.

In the case of using the SMDTMed2014, the AMC and the NAC are also evident, while the BSW outflow is absent. Similar to the ocean surface circulation calculated by the new regional MDT models, the systems of the CC, the RC, the PA and the MMA are also evident, with the addition of Ierapetra Anticyclone (IA) and of another anticyclone around the island of Samothrace (SA). Last but not least, we note a current that runs from the PA and extends across the west coast of Greece in Ionian Sea (Ionian Current, IC), as well as a system of currents coming from Aegean Sea and, through the straits between the islands of Crete and Kythira, outflowing to Mediterranean Sea.

3.1.4 The MDTCNES-CLS13 model

The MDTCNES-CLS13 model (Fig. 7 and Tab. 1 & Tab. 2) refers to the same 1993-2012 epoch and is based on a mixed geodetic-oceanographic methodology for the estimation of the MDT. In its geodetic part, it makes a first guess of the MDT at large scales by using the combination of the EGM-DIR-R4 geoid model, which is based on satellite data of 2 years only of the GOCE satellite mission and 7 years of the GRACE satellite mission, with the CNES-CLS11 Mean Sea Surface model, which is based on 20 years satellite altimetry observations. Then, it applies a synthesis method, where the model refines the first guess of the MDT with the use of purely oceanographic data, such as: (i) an updated catalogue with velocities of drifting buoys for the 1993-2012 epoch, (ii) an improved Ekman model for calculating the geostrophic component of the speed of the floating recorders and (iii) an updated list of the dynamic heights for the 1993-2012 epoch calculated from temperature/salinity profiles.

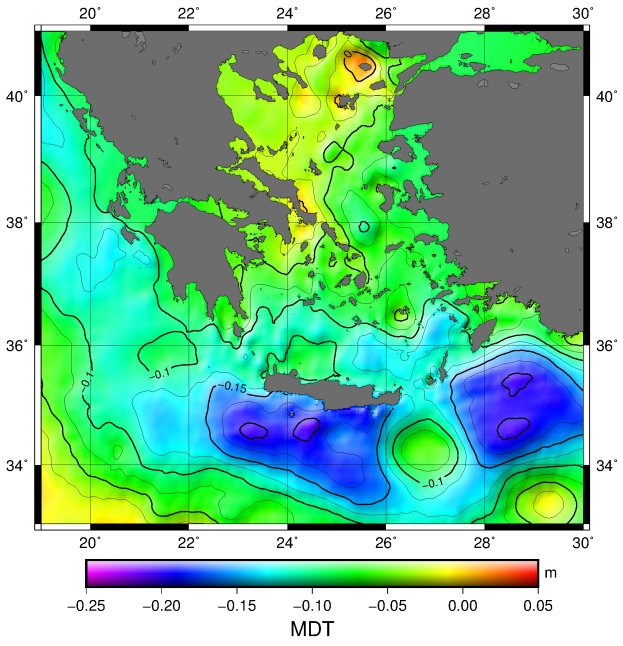

(a)

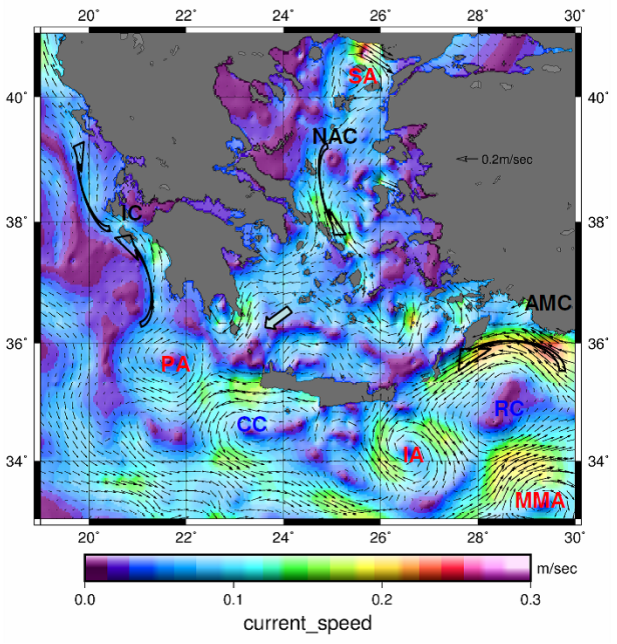

(b)

Fig. 6. (a)The heights of the SMDTMed2014 model. (b) The geostrophic ocean surface circulation as calculated by the SMDTMed2014 model.

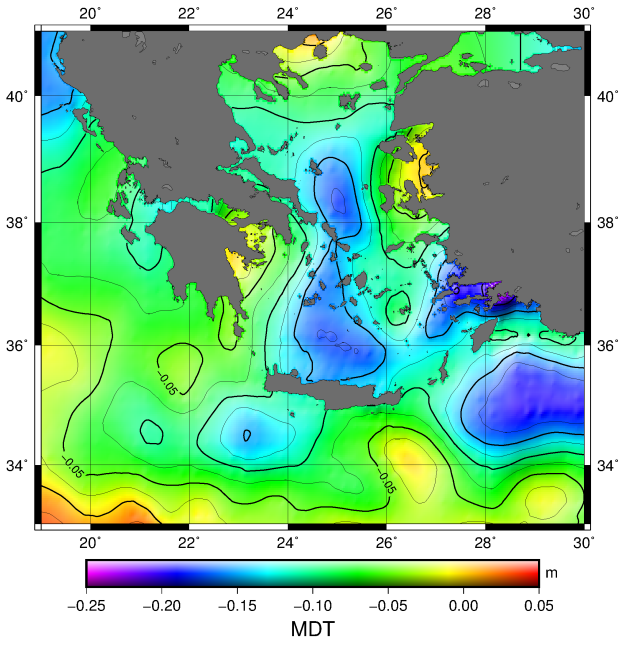

(a)

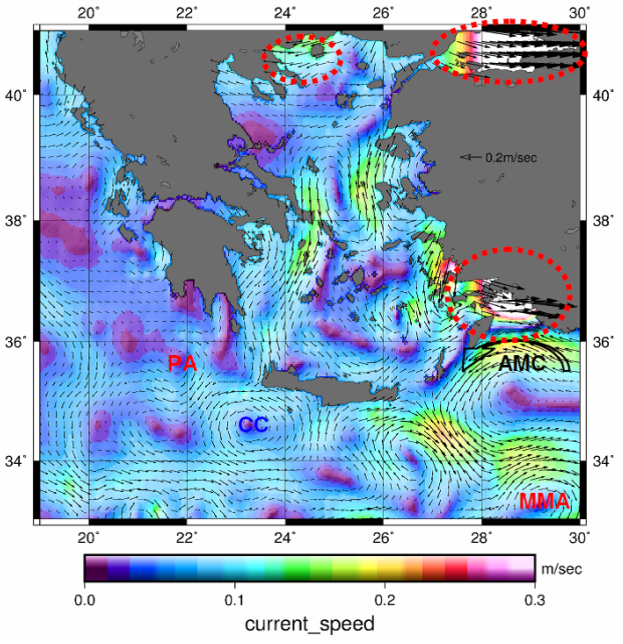

(b)

Fig. 7. (a) The heights of the MDTCNES-CLS13 model. (b)The geostrophic ocean surface circulation as calculated by the MDTCNES-CLS13 model.

The geostrophic ocean circulation, calculated by the MDTCNES-CLS13 model, also presents the AMC running across the southern coasts of the islands of Rhodes and Karpathos. In general, the large systems of the CC, the PA and the MMA, that are clearly noted in the previous models, are also observable but not with the same clarity and on the same locations. On the other hand, some strong currents are evident, which can be characterized as artifacts of the model. For example, alongside the northern band of the AMC and with an opposite direction to it, a very strong ocean surface current appears to flow across and in the southeastern coasts of Turkey, in the region of

the Halicarnassus peninsula. This ocean current is characterized as a model artifact, as it does not seem to relate to the rest of the ocean surface circulation and, in some parts, it seems to flow almost straight to the coast. Similarly, another strong current that is considered a model artifact is observed within Marmara Sea. In this case, the model presents a high velocity flow of the ocean surface of Marmara Sea in a uniform way and straight to its eastern coasts. In the same manner, another current, that is possibly an artifact of the model, is present in the northern part of Aegean Sea, that flows straight into the Strymonic gulf.

3.1.5 The DTU10MDT model

The DTU10MDT model (Fig. 8 and Tab. 1 & Tab. 2) follows a purely geodetic approach for the calculation of the MDT (Andersen and Knudsen, 2009). For its calculation, the DTU10 MSS surface (Andersen and Knudsen, 2010) is used, in conjunction with the EIGEN-6C geoid model (Förste et al, 2011). Regarding the DTU10MSS surface, appropriate filtering techniques are applied, in order to maintain the characteristics at short wavelengths and close to the coastlines. For the EIGEN-6C geoid model, the data come from the GOCE and the GRACE satellite gravity missions, in conjunction with gravity data on the Earth's surface and gravity data on the ocean surface derived from satellite altimetry, for enhancing the geoid signal at its shorter wavelengths. The true resolution of the DTU10MDT surface is defined by the isotropic Gaussian cutoff filter applied during the calculations that has an average width (at average power) of 0.75 degrees, which is close to 80 km.

The DTU10MDT model presents an ocean surface circulation that is in contrast to the well-known circulation of the case study area. Furthermore, it presents cases of very strong currents close to the coast and in closed gulfs that can be described as artifacts of the model. Such cases are: the strong currents depicted in Marmara Sea, in the western gulf of Corinth, in the Thermaic gulf and in the Turkish coasts east of the Rhodes island. Since the DTU10MDT model implements the geodetic approach, it calculates the MDT as the difference between the surfaces of the MSS and the geoid. Thus, its errors should be attributed to errors of one or both of these two surfaces. The precision of the DTU10MSS surface for the open ocean (for distances up to 50 km from the coastline) is estimated at the level of 2-3 cm (Mintourakis, 2014). Thus, the errors on the surface of the DTU10MDT model are more likely due to omission and commission errors of the EIGEN-6C geoid, or even to errors when applying the isotropic Gaussian cutoff filter and, to a smaller extent, to errors of the DTU10MSS close to the coasts.

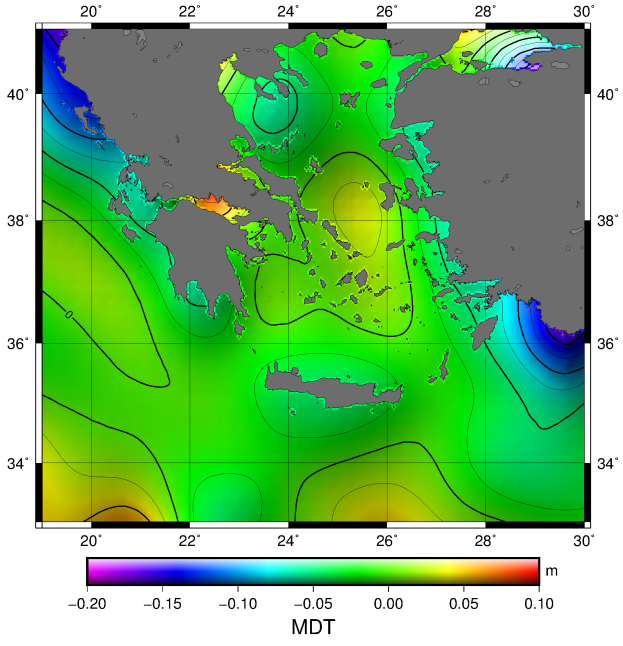

(a)

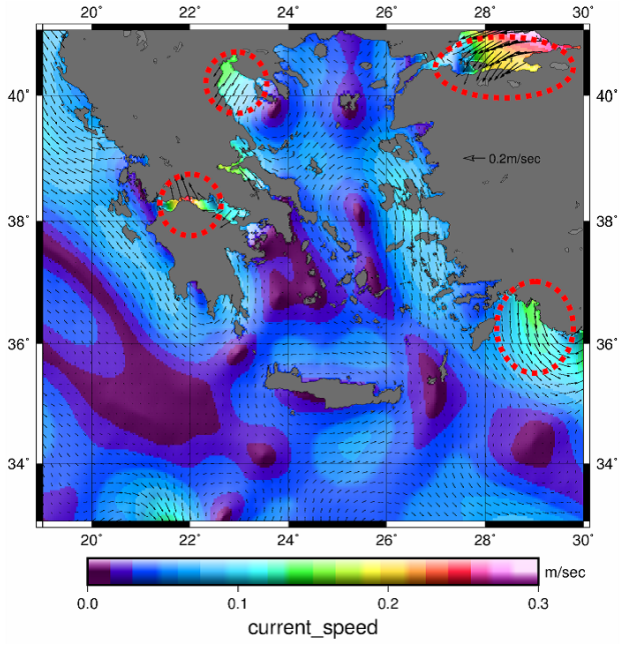

(b)

Fig. 8. (a) The heights of the DTU10MDT model. (b) The geostrophic ocean surface circulation as calculated by the DTU10MDT model.

3.2 Remarks on comparisons among the MDT models

From the analysis of the statistics of the surfaces and of the velocities of the geostrophic ocean surface currents for all five MDT models (Tab.1 and Tab.2), some findings are worth mentioning. First of all, the average value of the MDT differs significantly from model to model. In detail, the mean value of the MDT ranges from –0.017 m for the DTU10MDT model, to –0.212 m for the MSprMDT model, while the SMDTMed2014 and MDTCNES-CLS13 models present similar mean values for the MDT (–0.098 m and –0.089 m, respectively). These variations in the mean value of the elevation of the MDT models can be possibly attributed to the different MDT 'datum values' adopted by each model and to differences in the epoch that each model is referred to[2]. The values of the range and of the standard deviation of the MDT surface elevations are in agreement between all models (the ranges vary from 0.219 m to 0.265 m and the standard deviations vary from 0.034 m to 0.050 m). However, there are differences in the morphology of the MDT surfaces presented by each model. Specifically, the first three models, which implement a purely oceanographic approach for the calculation of the MDT, present a similar morphology and a generally positive slope of the MDT surface from Mediterranean Sea to Aegean Sea. In contrast, the other two models, which follow either the geodetic approach (DTU10MDT) or the mixed type approach (MDTCNES-CLS13) for the calculation of the MDT, present different morphologies to the three 'oceanographic' models and between them. In order to support these last findings with some numerical values we proceeded to a quantitative comparison. To do so, we choose the SMDTMed2014 to serve as a reference model and calculated the differences of all other MDT models with respect to this one. The statistics of the standard deviation and of the range of the differences (Tab. 3) present a better agreement of the new MDTs to the reference MDT. This is expected as long as i) the new MDTs and the reference MDT represent the oceanographic approach and ii) it numerically confirms the aforementioned morphological similarities. Regarding the values of the statistical parameters of the velocity of the geostrophic currents and of their U & V components (Tab. 2), there are no great differences between the MDT models but there are noticeable differences in the patterns of the ocean surface circulation they depict. The first three 'oceanographic' solutions of the MDT present surfaces with great similarities and a similar ocean surface circulation. Thus, they depict the well-known large-scale currents and cyclonic/anti-cyclonic systems in the area in an almost identical way and present similar circulation characteristics of smaller scale. On the other hand, the 'mixed type' implementation of the MDT depicts some of the large-scale currents and cyclonic/anti-cyclonic systems of the area but also presents some artifacts in the ocean surface circulation close to the coasts. Finally, the 'geodetic' implementation of the MDT does not represent any known features of the regional ocean surface circulation and is full of artifacts.

4 Validating the accuracy of the Ocean forecasting models

We now present comparisons of the DOT solutions of the above models with independent data, in order to evaluate their accuracy. The purpose of these comparisons is to provide an estimate of the accuracy level of the MDT for the Greek seas as determined by applying the oceanographic approach. Having a measure of this accuracy, and having studied the accuracy of the MSS models in the case study area (Mintourakis 2010, 2014), we are able to estimate the expected accuracy of the marine geoid for the case study area. In this context, the comparisons carried out in the Greek seas are: (i) on points located at the shoreline, where there are tidal records of monthly mean sea level values, (ii) across the surface area with gridded satellite altimetry monthly mean SLA values and (iii) along satellite altimetry tracks with SSH observations. For the above (i) and (ii) cases, there are datasets covering an extended period of time (at least since 1992) that refer to monthly mean values. Thus, the comparisons are made with the MFSpa monthly mean DOT solutions. On the other hand, case (iii) refers to comparisons that require a forecasting system that provides solutions at very high resolution, such as the 6 hours mean DOT solutions of the POSEIDON forecasting system.

4.1 Comparisons to tide gauge records

For these comparisons, we used the time series of the monthly mean sea level values at 12 tide gauge sites (Fig. 1), as provided by the Permanent Service for Mean Sea Level (Holgate et al., 2013; PSMSL, 2018) for a 19 years period, extending from 1993 to 2012. These monthly mean sea level values were calculated by the high rate (usually hourly) records of the tide gauges. The recorded level refers to an

2 There is no need to further investigate the origin of these variations in the present study but it is essential that these should be clarified in the case of geodetic applications.

Table 1. The statistics of the MDT elevations for all the models. Regarding the MSprMDT model the statistics of the MDT elevations are also presented in brackets for the 2008-2011 epoch in order to compare directly with the POSnaMDT model.

MDT elevations					
(m)	min	max	range	mean	std
MSprMDT (full epoch)	-0.313	-0.094	0.219	-0.212	0.038
MSprMDT (epoch 2008-2011)	(-0.308)	(-0.080)	(0.228)	(-0.208)	(0.043)
POSnaMDT	-0.318	-0.064	0.254	-0.176	0.050
SMDTMed2014	-0.213	0.021	0.234	-0.098	0.047
MDTCNES-CLS13	-0.232	0.033	0.265	-0.089	0.046
DTU10MDT	-0.177	0.086	0.263	-0.017	0.034

Table 2. The statistics of the current velocity components for all the models.

current velocity components						
	($m \cdot sec^{-1}$)	min	max	range	mean	std
MSprMDT	U	-0.493	0.384	0.877	0.007	0.065
	V	-0.336	0.413	0.749	-0.007	0.046
	total	-	0.594	0.594	0.063	0.050
POSnaMDT	U	-0.356	0.401	0.757	-0.003	0.073
	V	-0.309	0.281	0.590	-0.001	0.050
	total	-	0.392	0.392	0.069	0.054
SMDTMed2014	U	-0.213	0.255	0.468	0.005	0.065
	V	-0.206	0.161	0.368	-0.006	0.050
	total	-	0.306	0.306	0.069	0.045
MDTCNES-CLS13	U	-0.199	0.868	1.067	0.021	0.085
	V	-0.299	0.173	0.473	-0.013	0.054
	total	-	0.868	0.868	0.080	0.065
DTU10MDT	U	-0.293	0.127	0.419	0.012	0.040
	V	-0.186	0.235	0.421	-0.014	0.038
	total	-	0.294	0.294	0.047	0.033

Table 3. The statistics of the differences of the MDT elevations of each model to the reference model (SMDTMed2014).

MDT elevation differences					
(m)	min	max	range	mean	std
MSprMDT	-0.214	-0.031	0.183	-0.112	0.031
POSnaMDT	-0.230	0.010	0.240	-0.080	0.032
MDTCNES-CLS13	-0.180	0.120	0.300	0.011	0.051
DTU10MDT	-0.121	0.198	0.320	0.083	0.052

arbitrarily set zero altitude and, in most cases, there are no geodetic campaigns for monitoring any vertical displacements.

It is obvious that it is not possible to directly compare the DOT values provided by the OM with the monthly mean sea level values of the tidal records, as they do not refer to a common altitude scale. Given that, at a specific point *p,* there is a Tide Gauge (*TG*) and that the values of the DOT_p are available for a long period of time (as in the case of the MFSpr OGCM for the time period 1993-2012), the monthly values of the SLA's can be calculated from the OM, SLA_{MOD}, at point *p* for each month *m* as:

$$SLA_{MOD(p,m)} = DOT_{p,m} - MDT_p$$

where MDT_p is the mean value of all the DOT gridded solutions provided by the OM for the reference period (1993-2012), interpolated at the point p, while $DOT_{p,m}$ is the monthly mean DOT solution of the OM computed at the *p* point for the month *m*. The monthly values of the SLA at point *p*, where the TG is located, can also be calculated from the time series of the monthly sea-level values as:

$$SLA_{TG(m)} = SL_m - MSL_{TG}$$

where MSL_{TG} is the Mean Sea Level as calculated at the TG from records of the reference period (1993-2012), while SL_m is the monthly mean SL at the TG for the month m, as provided by the PSMSL. In this way, two time series of monthly SLAs are created for each TG site, the SLA_{MOD} derived from the OM and the SLA_{TG} derived from the TG records (Fig. 9). This is a demanding comparison, as it assesses an OM's ability to resolve the sea level variability on its boundaries at points over the coastline (Table 4). It is also extremely useful, as it relates to the ability of the OM to attribute the

value of the MDT at TG sites, contributing in vertical datum unification projects. In order to further investigate the differences of the two time series, we introduced a third time series in the comparisons for the site of each TG station using data derived from observations of satellite altimetry (Tables 5 & 6).

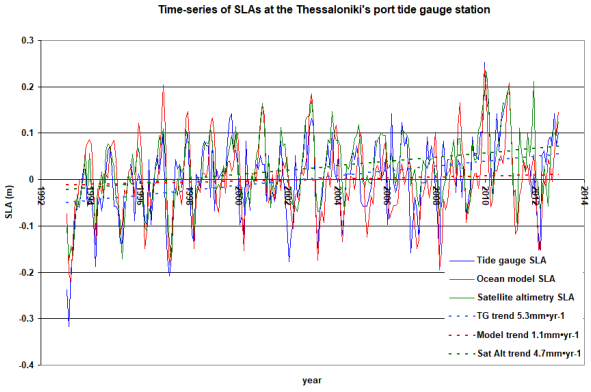

Fig. 9. The time-series derived i) by the DOT solutions of the MF-Spr OGCM and its corresponding sea level trend (red solid and dashed lines), ii) by the TG records and its corresponding sea level trend (blue solid and dashed lines), and iii) by the satellite altimetry data and its corresponding sea level trend (green solid and dashed lines), for the TG station located at Thessaloniki port in North Aegean Sea.

Almost all the charts of the time-series comparisons at the tide gauge stations present an image similar to that depicted for the case of the Thessaloniki tide gauge station (Fig. 9). From these charts we find that there is a satisfactory agreement on the sea level trends estimated by the time-series of the TG records and the Satellite Altimetry (SA) data (which have a mean value, for the 12 test sites, of 5.4 mm·yr^{-1} and 4.3 mm·yr^{-1}, respectively) while the corresponding trends, estimated by the time-series of the OM solutions (with a mean value of 1.3 mm·yr^{-1} for the 12 test sites), seem to underestimate the magnitude of the trend of the increasing sea level (Table 7).

The high value of the variance (8.7) and some extreme values of the sea level trends, estimated by the TG time-series, make us skeptical about the quality of the tide gauge records. The extreme values of sea level trends may result from biases introduced in the TG time-series by any possible vertical displacements of the plate, at which each TG station is based. Such vertical displacements can be due to geodynamical phenomena and/or due to local phenomena (e.g. sedimentation of the tiller pad). As the comparisons are held for an extended period of time (19 years), such phenomena are quite possible (especially for an active tectonic region such as the case study area and for tide gauge stations placed in ports) and this raises the question of the suitability of these TG records for such comparisons. Taking into account that there are no geodetic campaigns for monitoring vertical displacements of the tide gauge sites, the only available option to get an estimate of such phenomena (at least those that are of a geodynamical nature) is the use of elevation time-series by any available nearby GNSS station. In our case, the GNSS elevation time-series are provided by various institutions, such as the Nevada Geodetic Laboratory (Blewitt et al., 2018), Système d'Observation du Niveau des Eaux Littorales (Wöppelmann, 2004) and the EUREF Permanent Network (Bruyninx et al., 2001). If the vertical velocity of the GNSS station is not provided by the corresponding institution, we make a rough estimate by its elevation time-series. In this way, we compare the vertical velocity estimated by the GNSS site to the vertical velocity of a TG station by the differences:

$$VV_{TG-OM} = SLT_{TG} - SLT_{SA}$$

and

$$VV_{TG-SA} = SLT_{TG} - SLT_{OM}$$

where SLT_{TG}, SLT_{SA} and SLT_{OM} are the sea level trends estimated by the time-series of the TG records, of the OM solutions and of the SA data, respectively (Table 8).

We should mention that the estimated vertical velocities of the GNSS stations are derived from elevation time-series at epochs different than the epochs of the TG, OM and SA sea level time-series. Thus, these results are presented only in order to give a rough estimate of the precision that the tide gauge sea level time-series can provide in such comparisons and the problems that have to be accounted for before reaching conclusions. Despite the likelihood of errors in the TG time-series, the level of their accuracy still allows for some initial conclusions to be drawn.

Therefore, based on the results of these point comparisons, we find that the OM is able to accurately capture the phases and the amplitudes of the sea level variations at points on the shore. We consider that the values of the statistics for the differences between the OM results and the TG records, as well as the satellite altimetry data, present a satisfactory agreement. Specifically, the agreement of the OM DOT solutions to the satellite altimetry data is better than that to the TG records, since they present a stronger correlation (0.78 versus 0.61) and a smaller value of the standard deviation of their differences, 5.1 cm versus

Table 4. The statistics for the differences between the SLA timeseries derived by the TG records and the OM solutions, and their correlation at each TG site. The average value of the st.dev and of the correlation for all the 12 test sites is 0.072m and 0.61 respectively.

	SLA_{TG} - SLA_{MOD}					
Tide gauge site	mean (m)	st.dev. (m)	min. (m)	max. (m)	range (m)	correlation
Alexandroupolis	-0.002	0.067	-0.178	0.172	0.350	0.640
Iraklio (Isl. Crete)	-0.005	0.102	-0.280	0.253	0.533	0.454
Thessaloniki	0.002	0.070	-0.188	0.212	0.400	0.667
Kavala	0.001	0.083	-0.247	0.180	0.427	0.436
Kalamata	0.000	0.061	-0.174	0.136	0.311	0.746
Katakolo	0.000	0.061	-0.189	0.144	0.332	0.707
Isl. Leros	-0.003	0.063	-0.164	0.110	0.274	0.575
Isl. Lefkada	0.005	0.077	-0.179	0.171	0.350	0.696
Piraeus	0.000	0.078	-0.227	0.168	0.395	0.596
Soudha (Isl. Crete)	0.000	0.068	-0.194	0.192	0.386	0.683
Isl. Syros	0.000	0.069	-0.212	0.136	0.348	0.636
Isl. Chios	0.001	0.071	-0.204	0.224	0.428	0.505

Table 5. The statistics for the differences between the SLA timeseries derived by the OM solutions and the satellite altimetry data, and their correlation at each TG site. The average value of the st.dev and of the correlation for all the 12 test sites is 0.051 m and 0.78 respectively.

	$SLA_{SAT} - SLA_{MOD}$					
Tide gauge site	mean (m)	st.dev. (m)	min. (m)	max. (m)	range (m)	correlation
Alexandroupolis	0.029	0.052	-0.110	0.135	0.245	0.775
Iraklio (Isl. Crete)	0.028	0.052	-0.136	0.185	0.321	0.784
Thessaloniki	0.025	0.055	-0.106	0.158	0.264	0.779
Kavala	0.028	0.053	-0.110	0.168	0.277	0.772
Kalamata	0.029	0.050	-0.090	0.146	0.235	0.815
Katakolo	0.029	0.046	-0.100	0.129	0.229	0.816
Isl. Leros	0.029	0.056	-0.146	0.152	0.298	0.710
Isl. Lefkada	0.029	0.047	-0.092	0.133	0.225	0.808
Piraeus	0.028	0.049	-0.096	0.144	0.240	0.789
Soudha (Isl. Crete)	0.030	0.051	-0.129	0.149	0.278	0.771
Isl. Syros	0.029	0.048	-0.097	0.153	0.251	0.793
Isl. Chios	0.029	0.050	-0.097	0.143	0.240	0.775

7.2 cm (Table 4 & Table 5). The corresponding comparisons between the SLA time-series derived by the TG records and the satellite altimetry data are also provided (Table 6) and they present a correlation of 0.74 and a value of 5.5 cm for the standard deviation of their differences. In any case, it is clear that the OM achieves an accuracy of 5-7 cm in estimating the sea level variations for a 19-year long period of time at points on the coastline. This also implies a similar accuracy in calculating the value of the MDT at these points. Although the number of test points is small (12 TG stations) in order to support the conclusion that the accuracy will be at the same level across the coastlines of the entire region, the spatial distribution of the comparisons, which cover a great extent of the area, and their results, which do not differ significantly from site to site, indicate that the accuracy across the coastlines for the case study area should be at about the presented level. Regarding the sea level trend comparisons, it is possible that the OM underestimates the value of the sea level trend, something that is evident in the following comparisons with satellite altimetry data.

4.2 Comparisons to altimetry data

In order to further investigate the accuracy of the OM in providing sea level variations, we make comparisons with satellite altimetry gridded SLA and along track SSH data sets in the full extent of the case study area.

4.2.1 Comparisons with gridded SLA data sets

The gridded SLA data sets were generated by post-processing the SSH observations of multiple satellite altimetry missions, processed and distributed for Mediterranean Sea by the Copernicus Marine and Environment

Table 6. The statistics for the differences between the SLA timeseries derived by the TG records and the satellite altimetry data, and their correlation at each TG site. The average value of the st.dev and of the correlation for all the 12 test sites is 0.055m and 0.74 respectively.

	$SLA_{TG} - SLA_{SAT}$					
Tide gauge site	mean (m)	st.dev. (m)	min. (m)	max. (m)	range (m)	correlation
Alexandroupolis	-0.030	0.050	-0.174	0.096	0.270	0.739
Iraklio (Isl. Crete)	-0.031	0.073	-0.201	0.144	0.345	0.763
Thessaloniki	-0.023	0.055	-0.200	0.140	0.340	0.777
Kavala	-0.024	0.070	-0.200	0.163	0.363	0.501
Kalamata	-0.028	0.049	-0.164	0.087	0.251	0.826
Katakolo	-0.030	0.047	-0.209	0.072	0.281	0.770
Isl. Leros	-0.030	0.055	-0.172	0.096	0.267	0.611
Isl. Lefkada	-0.027	0.060	-0.203	0.132	0.335	0.772
Piraeus	-0.032	0.058	-0.198	0.094	0.292	0.746
Soudha (Isl. Crete)	-0.029	0.044	-0.150	0.098	0.248	0.855
Isl. Syros	-0.029	0.047	-0.175	0.073	0.248	0.841
Isl. Chios	-0.029	0.053	-0.180	0.214	0.394	0.654

Table 7. The sea level trends estimated by the time-series of i) the DOT solutions of the OM, ii) the TG monthly mean sea level records, and iii) the SA data at each TG station.

	sea level trend ($mm \cdot yr^{-1}$)		
Tide gauge site	OM	TG	SA
Alexandroupolis	1.2	4.4	4.3
Iraklio (Isl. Crete)	1.9	9.5	5.8
Thessaloniki	1.1	5.3	4.7
Kavala	1.3	1.8	4.0
Kalamata	1.8	5.2	5.3
Katakolo	1.5	5.7	3.6
Isl. Leros	0.7	0.9	2.5
Isl. Lefkada	0.9	10.4	2.5
Piraeus	1.1	8.1	5.0
Soudha (Isl. Crete)	2.0	6.7	5.3
Isl. Syros	0.9	3.9	4.0
Isl. Chios	1.0	2.5	4.1
Statistics of the above sea level trends			
mean value	1.3	5.4	4.3
variance	0.2	8.7	1.1

Monitoring Service (CMEMS) and described as the Delayed Time Map of the SLAs (DT-MSLA). These DT-MSLA data are available for the case study area since January 1993, thus the comparisons to the MFS-OCM were held for the exact epoch as for the comparisons to the TG records (January 1993 to December 2012). As in the previously presented case of the point comparisons to TG records, the monthly mean of the SLA at each grid node, with longitude i and latitude j, can be calculated from the monthly mean of the DOT solutions of the MFS-OCM grids for each month m by:

$$SLA_{OM_{i,j,m}} = DOT_{i,j,m} - MDT_{i,j} \quad (1)$$

where $MDT_{i,j}$ is the average of all monthly values of the DOT solutions of the MFS-OCM for the reference epoch (1993-2012) at the grid node, with longitude i and latitude j, and $DOT_{i,j,m}$ is the DOT solution of the MFS-OCM for that grid node at the m month. On the other hand, the DT-MSLA data set, computed from multiple satellite altimetry missions, provides the monthly SLA values for each i, j grid node of the case study area and for each m month of the reference epoch (1993-2012), hereafter noted as SLA_{SA}. In this way, two monthly mean SLA grids are available for each month m, the SLA_{OM} grid and the SLA_{SA} grid. Thus, the accuracy of the MFS-OCM in providing the sea level variations is evaluated by computing the differences $\Delta_{i,j,m}$ between the two monthly mean SLA grids at each i, j grid node throughout the extent of the case study area for each m month of the 1993-2012 epoch as:

$$\Delta_{i,j,m} = SLA_{OM_{i,j,m}} - SLA_{SA_{i,j,m}} \quad (2)$$

For each m month we calculate the mean and the standard deviation values of the $\Delta_{i,j,m}$ differences and present their

Table 8. The vertical velocities *TG-OM*, *TG-SA* calculated by the differences between the time-series derived by i) the DOT solutions of the OM, ii) the TG monthly mean sea level records, and iii) the satellite altimetry data with respect to the vertical velocities estimated by the time-series of heights provided by nearby GNSS stations. The TG, OM and SA data refer to time series covering the same period from 1993 to 2012, while the GNSS data (wherever and whenever available) refer to time series of different epochs.

	vertical velocities (mm·yr^{-1})		
Tide gauge site	**TG-OM**	**TG-SA**	**GNSS (Site ID, epoch)**
Alexandroupolis	**-3.2**	**-0.1**	**n.a.[3]**
Iraklio (Isl. Crete)	**-7.6**	**-3.7**	**-0.8 (HERA, 2010.36-2016.40)**
Thessaloniki	**-4.2**	**-0.6**	**-1.6 (AUT1, 2005.25-2016.02)**
Kavala	**3.1**	**2.2**	**1.1 (KAV1, 2010.69-2016.10)**
Kalamata	**-3.4**	**0.1**	**0.2 (KALM, 2010.84-2016.40)**
Katakolo	**-4.2**	**-2.1**	**1.1 (PYRG, 2011.56-2016.40)**
Isl. Leros	**-0.2**	**1.6**	**n.a.**
Isl. Lefkada	**-9.5**	**-7.9**	**-1.3 (SPAN, 2007.39-2012.01)**
Piraeus	**-7.0**	**-3.1**	**0.6 (NOA1, 2006.02-2018.70)**
Soudha (Isl. Crete)	**-4.7**	**-1.4**	**0.0 (TUC2, 2004.74-2010.53)**
Isl. Syros	**-3.0**	**0.1**	**n.a.**
Isl. Chios	**-1.5**	**1.6**	**n.a.**

variation over the 1993-2012 epoch Fig. 10 & 11).The vertical velocities *TG-OM*, *TG-SA* calculated by the differences between the time-series derived by i) the DOT solutions of the OM, ii) the TG monthly mean sea level records, and iii) the satellite altimetry data with respect to the vertical velocities estimated by the time-series of heights provided by nearby GNSS stations. The TG, OM and SA data refer to time series covering the same period from 1993 to 2012, while the GNSS data (wherever and whenever available) refer to time series of different epochs.

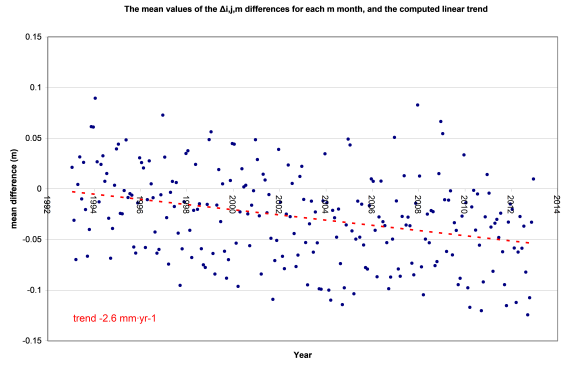

Fig. 10. The variation of the mean values of the $\Delta_{i,j,m}$ differences for each m month over the 1993-2012 epoch and the computed linear trend (red dashed line).

From Fig. 10, it is evident that the mean values of the $\Delta_{i,j,m}$ differences for the 1993-2012 epoch present a linear trend, drifting from 0 cm, at the beginning of the epoch, up to −5.5 cm at the end of the epoch. By fitting a linear model, the value of the trend is estimated as -2.6 mm·yr^{-1}. This confirms the finding, stated during the point comparisons at TG sites, that the MFS-OCM possibly underestimates the value of the sea level trend and further research is needed in order to investigate the possible causes.

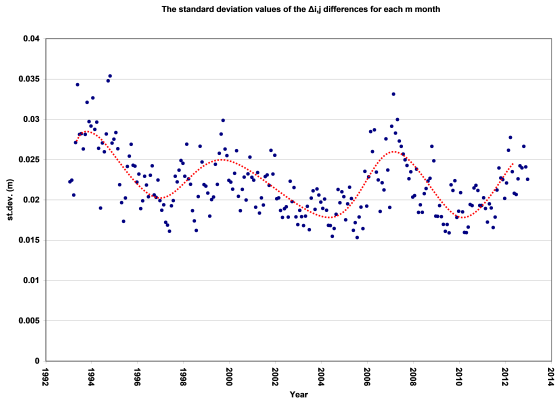

Fig. 11. The variation of the standard deviation values of the $\Delta_{i,j,m}$ differences for each m month over the 1993-2012 epoch. The red dotted line highlights the observed periodicity.

From Fig. 11, it is observed that the standard deviation values of the $\Delta_{i,j}$ differences for each m month present a small value, ranging from 1.5 cm to 3.5 cm. This highlights a good agreement between the monthly SLA gridded solutions computed by the MFS-OCM and by the satellite altimetry. Nevertheless, it looks like that the monthly standard deviation values are not randomly scattered in time

3 not available

but they present a periodicity pattern in their fluctuation. This observed periodicity corresponds to a period of 6-7 years and an amplitude of 1.5 cm. This suggests that there are epochs of better agreement between the SLA grids calculated from the MFS-OCM and the SLA grids that are derived from the satellite altimetry SSH observations and needs further investigation. A possible cause is the existence of a periodic phenomenon, such as the interchange between cyclonic and anticyclonic circulation in the Ionian Sea Basin (Bessieres et al., 2012), which is not sufficiently described by the MFS-OCM, resulting in solutions of a lower precision during the phenomenon.

4.2.2 Comparisons to along track SSH data sets

In some geodetic problems the DOT elevations must be provided accurately, with satisfactory spatial and temporal resolution, in order to apply the necessary reductions of the SSH observations to the geoid. Such cases arise when the SSH observations (mostly obtained by ship-borne GPS or airborne altimetry) are used:

1. for local marine geoid modeling (Limpach, 2010; Mintourakis, 2010)
2. to connect the vertical datums of two (or more) TG stations[4]
3. to connect the vertical datum of a TG site on the coastline to a Mean Sea Level profile in the open ocean that is obtained after the averaging of multiple SSH observations on the repeated track of an exact repeat satellite altimetry mission

and the complex hydrodynamics of the region does not allow to simply extrapolate the local marine geoid slope (obtained only by the SSH observations) from one site to another (or between offshore altimetric measurements to the coastal tide gauge locations). In such cases it is necessary to have an OM that provides the DOT elevations with the highest possible spatial and temporal resolution, suitable for the reduction of these SSH observations to the geoid surface.

In this section, we want to examine the accuracy of the high-frequency solutions of the POS-POM model, in order to investigate their possible use in the reduction of instantaneous SSH observations to the geoid. Therefore, we proceeded to making further tests regarding the POS-POM, as it is the only ocean model that provides the DOT elevations in high resolution (at periods of 6 hours) for the case study area. The tests were done by comparing these high resolution solutions of the DOT, provided by the POS-POM, with the solutions of the DOT calculated with the use of satellite altimetry SSH observations and a regional geoid model. The SSH observations were derived from the Jason-2 satellite altimetry mission, were optimized for coastal environments and distributed under the Coastal and Hydrological (PISTACH) products of the AVISO-CNES data centre (Mercier et al., 2008). The comparisons were made using the 36 SSH profiles collected in 2009 by the Jason-2 altimeter, during the cycles from 18 to 54 over the satellite descending pass number 94. The satellite footprint during this descending pass was running from the 40^{th} parallel in North Aegean Sea to the 33^{rd} parallel in Cretan Sea, thus crossing the whole extent of the case study area from north to south. In order to compare these SSH profiles to the periodic solutions of the DOT grids computed by the POS-POM, we had to transform them to profiles of the DOT. To do so, we removed the geoid height N, calculated by the National Technical University of Athens Marine Geoid model version 1 (NTUAMGv1[5]) regional model (Mintourakis, 2014) from the SSH observed by the satellite altimeter at each point p for each of the 36 profiles:

$$DOT_{SA_p} = SSH_p - N_p \tag{3}$$

where N_p is the geoid height calculated by interpolating the height values of the NTUAMGv1 regional model at each point p. Then we interpolated the value of the DOT, calculated by the POS-POM model, at each point p of each profile. In this way we obtained 36 pairs of DOT profiles for comparisons along track the satellite's descending pass number 94 (Fig. 12). It should be noted that, for every profile, we picked the DOT grid of the POS-POM's periodic solution that is closer to the time of the satellite's pass.

For each point p of each of the 36 profiles, we calculate the differences:

$$\Delta_p = DOT_{OM_p} - DOT_{SA_p}$$

where DOT_{OM} and DOT_{SA} are the values of the DOT for the point p calculated by the POS-POM and by the Satellite

4 For example, there might be a case when trying to connect the vertical datums of two (or more) TG stations, the only available data are a unique trajectory (of airborne or ship-borne GPS altimetry) SSH observations between the two stations. These SSH observations take place within a short period of time, ranging from a few minutes (for the case of the airborne altimetry) to some hours (in the case of ship-borne GPS altimetry).

5 The NTUAMGv1 is a marine geoid model computed in an oceanographic approach after subtracting the Synthetic Mean Dynamic Topography RIO07 MDT model (Rio et. al., 2007) from the National Technical University of Athens Mean Sea Surface v1 model (NTUAMSSv1). The NTUAMSSv1 is generated purely by satellite altimetry SSH observations.

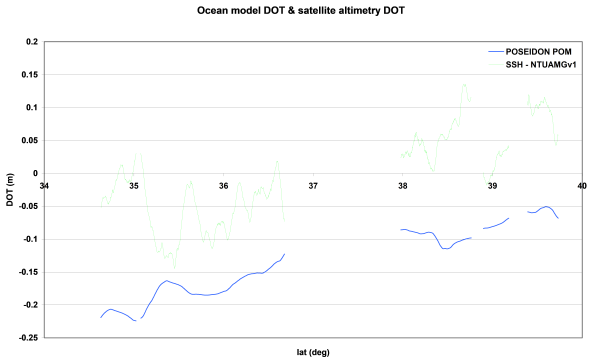

Fig. 12. A pair of the DOT profiles as computed i) by the POS-POM (blue line) and ii) by the altimetric approach (green line) along track the Jason-2 satellites footprint during it's descending pass over the track number 94 at it's 44th cycle.

Altimetry data set, respectively. After calculating these Δ_p differences, we compute the mean value and the standard deviation value for the profile of each cycle number and we present the corresponding graphs (Fig. 13).

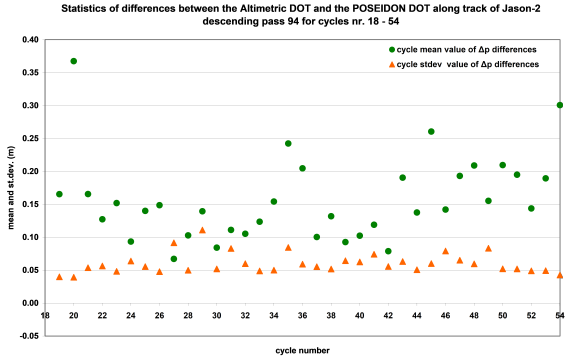

Fig. 13. The mean value and the standard deviation value of the Δ_p differences between the DOT values calculated by the POS-POM and by the Satellite Altimetry data set, over the Jason-2 satellite descending pass number 94 and during the cycle's number from 18 to 54.

Although the values of the standard deviation of the Δ_p differences are small (4 cm to 8 cm), we cannot draw any safe conclusion regarding the accuracy of the DOT solutions provided by the POS-POM because the signal of the DOT in the case study area is small and close to the precision of a satellite's altimeter, especially in coastal regions. This means that the satellite's altimeter SSH observations do not have the precision required to check the accuracy of the high rate (every 6-hours) DOT solutions of the POS-POM in the case study area. Therefore, we plan to make similar comparisons to ship-borne GPS SSH data sets, when the Poseidon's Live Access Server gets available for providing the POS-POM solutions to its users. These data sets refer to SSH observations collected by GPS receivers on board research vessels (Mintourakis, 2010) which have enough resolution to evaluate the solutions of highly detailed ocean models, such as the Dutch Continental Shelf Model version 6 (DCSMv6) (Zijl et al., 2013), which was used in connecting the vertical datums between island and mainland TG stations in Holland (Slobbe et al., 2018).

5 Conclusions

In the present study we computed two new surfaces of the MDT for the region of the Greek seas by averaging, for extended epochs, the gridded DOT solutions derived from two operational forecasting systems that implement different ocean circulation models. In order to evaluate the new regional MDT models, we made comparisons between them and three state-of-the-art models that represent the oceanographic, the geodetic, and the mixed type methodologies for the estimation of the MDT.

The numerical comparisons of the values of the MDT surfaces and of their velocity vector fields do not indicate with certainty which model, and therefore methodology, performs better than the others. Therefore, we extended the comparisons by interpreting the patterns of the ocean surface circulation presented by each model and validating it, based on well-known currents and cyclonic/anti-cyclonic systems of Eastern Mediterranean Sea. These comparisons revealed great similarities between the three models that implement the oceanographic approach. On the other hand, they revealed some issues of the MDT CLS13 model, which implements a mixed geodetic/oceanographic approach, and the weakness of the DTU10MDT model, which implements the geodetic approach. These findings highlight why it is critical, when comparing MDT models, to extend the comparisons up to the level of the interpretation of the calculated patterns of the geostrophic ocean circulation.

Furthermore, in order to validate the precision of the OM's to track the sea level variations, we performed numerous comparisons to tide gauge sea level records and to satellite altimetry gridded SLAs and along track SSH observations. These comparisons revealed a very good agreement between the SLAs computed by the tested ocean models and by the testing data sets, both for the coast line and for the open ocean test cases. Some issues with the MFS OGCM, which require further research, are: i) it under-

estimates the value of the sea level trend and ii) it presents some periods with solutions of a lower precision.

In Mediterranean Sea, where dense ocean observation networks, continuously updated data sets, a well-known bathymetry and atmospheric models to describe the ocean/atmosphere interaction are available, the ocean forecasting models can provide the solutions of the DOT in great detail and precision. From our tests on the ability of the OM's to track the SLA's, the results suggest that the implementation of the oceanographic approach for computing the MDT surface provides a precision at an estimated level of 2-5 cm. If we were to make similar tests in a vast ocean (e.g. the Pacific Ocean), the results would possibly be different, with the geodetic and the mixed type geodetic/oceanographic approaches of the MDT providing better results than the purely oceanographic implementation of the MDT. The present findings, regarding the utilization of the oceanographic approach for the implementation of the MDT, agree with similar research (Filmer et al., 2018) and highlight the need to further develop the geodetic infrastructures by actions such as the installation of GNSS receivers at the tide gauge stations and the realization of an airborne gravity campaign that will allow the realization of a gravimetric geoid with high resolution and precision. The above will provide additional control of ocean circulation models and will also contribute to a better synergy between the geodetic and the oceanographic approaches for the implementation of the MDT. In any case, as the convergence of the geodetic and the oceanographic MDT is a good indicator of accuracy for both approaches and facilitates their combination, it is still fundamental to improve the gravimetric geoid modeling along the coast (Huang, 2017) especially in non-ordinary cases like the Greek seas.

With regard to the issue of the realization of the same datum among the different OMs (or considering the issues of compatibility of the so called 'normal' values among an MDT model and a MSS), we need to clarify that, although it is of great importance, this is not included in the current work. Since this is a preliminary study, we did not address this issue during our experiments. Thus, the comparisons may be biased due to uncertainty of the vertical references of each model, the different time periods and details around interpolation to the tide gauges, plus the tide system used for the geodetic MDT. Therefore, the comparisons were made using the relative differences (SLA's) and not the absolute differences (DOT's /ADT's). This would be also a requirement on a purely geodetic project such as the LVD unification. Such a comparison or project requires further research to investigate the effects caused by the different datums and 'normal' values adopted by each model and surface. This can be a follow-on research, where, besides extending the comparisons to other geodetic MDTs and independent redundant data, it would be interesting to compare the estimates of the LVD offsets computed by the oceanographic approach to the ones already identified by the geodetic approach in related research (Kotsakis et al., 2012) for the case study area. Until then, one can conclude that the oceanographic approach provides an attractive alternative over the geodetic and the mixed type geodetic/oceanographic approaches for the implementation of the MDT in the case study area.

Finally, we emphasize that the use of ocean circulation models for the implementation of the MDT for geodetic applications offers some advantages, besides the precision of the computed DOT values, such as the uniformity of the geographic grids, the periodicity of their solutions and the continuity for extended epochs. Thus, the new MDT models can be easily updated by the continuous solutions of the operational forecasting systems and can be combined with synchronous MSS models, computed for the same epochs, in order to define a dynamic national/regional vertical datum that can be easily and continuously updated to more precise and extended versions.

Acknowledgements: The authors wish to thank Dr. D. Velaoras, researcher at the Hellenic Centre for Marine Research, for his valuable help regarding the description of the ocean circulation characteristics of the Greek seas and for his suggestions and comments in the preparation of the present study. In addition, several comments and suggestions made by Prof. R. Korakitis (SRSE/NTUA) are greatly appreciated. We also wish to thank Dr. Yan-Ming Wang of NGS-NOAA and the anonymous reviewers for their many helpful and constructive comments.

References

Andersen O.B. and Knudsen P., 2009, DNSC08 mean sea surface and mean dynamic topography models. J. Geophys. Res. Oceans, 114:C11001. https://doi.org/10.1029/2008JC005179

Andersen O.B., and Knudsen P., 2010, The DTU10 mean sea surface and mean dynamic topography – Improvements in the Arctic and coastal zone. Ocean Surface Topography Science Team (OSTST) 2010 meeting, Lisbon, Portugal, 18 - 20 October 2010.

Andersen, O.B., Nielsen, K., Knudsen, P., Hughes, C.W., Bingham, R., Fenoglio-Marc, L., Gravelle, M., Kern, M., and Padilla Polo S., 2018 Improving the Coastal Mean Dynamic Topography by Geodetic Combination of Tide Gauge and Satellite Altimetry, Marine Geodesy, vol.41:n.6, p.p.517-545, DOI: 10.1080/01490419.2018.1530320

Bingham R.J., Haines K., and Hughes C.W., 2008, Calculating the ocean's mean dynamic topography from a mean sea surface and a geoid, J Atmos. Ocean Technol. 25(10), 1808-1822, doi: 10.1175/2008JTECHO568.1

Bingham R.J., Haines K., and Lea D. J., 2014, How well can we measure the ocean's mean dynamic topography from space?, J. Geophys. Res. Oceans, 119, 3336–3356, doi:10.1002/2013JC009354.

Blewitt G., Hammond W.C., and Kreemer C., 2018, Harnessing the GPS Data Explosion for Interdisciplinary Science, Eos, 99, doi: 10.1029/2018EO104623

Blumberg, A.F., and Mellor G.L., 1987, A description of a three-dimensional coastal ocean circulation model, in Three-Dimensional Coastal Ocean Models, Vol. 4, Edited by N. Heaps, pp. 208, American Geophysical Union, Washington, D.C.

Bruyninx C., Becker M., and Stangl G., 2001, Regional Densification of the IGS in Europe Using the EUREF Permanent GPS Network, Phys. Chem. Earth, 26(6-8), 531-538.

Drinkwater, M.R., Floberghagen R., Haagmans R., Muzi D., and Popescu A., 2003. GOCE: ESA's first Earth Explorer Core mission. In Beutler, G.B., Drinkwater M., Rummel R., and von Steiger R. (Eds.), Earth Gravity Field from Space - from Sensors to Earth Sciences. In the Space Sciences Series of ISSI, Vol. 18, 419-432, Kluwer Academic Publishers, Dordrecht, Netherlands, ISBN: 1-4020-1408-2

Filmer S.M., Hughes C., Woodworth P.L., Featherstone W., and Bingham R.J., 2018, Comparison between geodetic and oceanographic approaches to estimate mean dynamic topography for vertical datum unification: evaluation at Australian tide gauges, Journal of Geodesy, 92, 1413-1437. doi: 10.1007/s00190-018-1131-5

Förste C., Bruinsma S., Shako R., Marty J-C, Flechtner F., Abrikosov O., Dahle C., Lemoine J-M., Neumayer K.H., Biancale R., Barthelmes F., König R., and Balmino G., 2011, EIGEN-6 - A new combined global gravity field model including GOCE data from the collaboration of GFZ Potsdam and GRGS-Toulouse, Geophysical Research Abstracts, Vol. 13, EGU2011-3242-2, EGU General Assembly.

Holgate S.J., Matthews A., Woodworth P.L., Rickards L.J., Tamisiea M.E., Bradshaw E., Foden P.R., Gordon K.M., Jevrejeva S., and Pugh J., 2013, New Data Systems and Products at the Permanent Service for Mean Sea Level. Journal of Coastal Research, 29(3), 493-504. doi: 10.2112/JCOASTRES-D-12-00175.1

Huang J., 2017, Determining coastal mean dynamic topography by geodetic methods, Geophysical Research Letters, 44, https://doi.org/10.1002/2017GL076020

Karageorgis A., Gardner W., Georgopoulos D., Mishonov A., Krasakopoulou E., and Anagnostou C., 2008, Particle dynamics in the Eastern Mediterranean Sea: A synthesis based on light transmission, PMC, and POC archives (1991-2001). Deep Sea Research Part I: Oceanographic Research Papers, 55, 177-202. 10.1016/j.dsr.2007.11.002

Korres G., and Lascaratos, A., 2003, A one-way nested eddy resolving model of the Aegean and Levantine basins: implementation and climatological runs, Ann. Geophys., 21, 205-220, doi: 10.5194/angeo-21-205-2003

Korres G., Lascaratos A., Hatziapostolou E., and Katsafados P., 2002, Towards an Ocean Forecasting System for the Aegean Sea. The Global Atmosphere and Ocean System, 8(2-3), 191-218.

Korres G., Nittis K., Hoteit I., and Triantafyllou G., 2009, A high resolution data assimilation system for the Aegean Sea hydrodynamics, Journal of Marine Systems ,77, 325-340

Kotsakis, C., Katsambalos, K. & Ampatzidis, D, 2012, Estimation of the zero-height geopotential level W_0^{LVD} in a local vertical datum from inversion of co-located GPS, leveling and geoid heights: a case study in the Hellenic islands, Journal of Geodesy, Vol.86, Issue 6, pp.423-439, https://doi.org/10.1007/s00190-011-0530-7

Knudsen P., and Andersen O.B., 2013, The DTU12MDT global mean dynamic topography and ocean circulation model. In: Proceedings of ESA Living Planet Symposium, European Space Agency.

Limpach, P., 2010, Sea Surface Topography and Marine Geoid by Airborne Laser Altimetry and Shipborne Ultrasound Altimetry. Geodätisch-geophysikalische Arbeiten in der Schweiz. Volume 80. Schweizerische Geodätische Kommission. ISBN 978-3-908440-24-6.

Madec G., Delecluse P., Imbard M., and Levy C., 1998, OPA 8.1 ocean general circulation model reference manual, Institut Pierre-Simon Laplace, Note du Pole de Modelisazion, No. 11, 91 pp.

Maximenko, N., Niiler, P., Centurioni, L., Rio, M., Melnichenko, O., Chambers, D., Zlotnicki, V. and Galperin, B., 2009, Mean Dynamic Topography of the Ocean Derived from Satellite and Drifting Buoy Data Using Three Different Techniques. J. Atmos. Oceanic Technol., 26, 1910–1919, https://doi.org/10.1175/2009JTECHO672.1

Mercier F., Dibarboure G., Dufau C., Carrere L., Thibaut P., Obligis E., Labroue S., Ablain M., Sicard P., Garcia G., Moreau T., Commien L., Picot N., Lambin J., Bronner E., Lombard A., Cazenave A., Bouffard J., Gennero M.C., Seyler F., Kosuth P., and Bercher N., 2008, Improved Jason-2 altimetry products for Coastal Zones and Continental Waters (PISTACH Project), Ocean Surface Topography Science Team, Nice, France, November 2008, http://www.aviso.oceanobs.com/fileadmin/documents/OSTST/2008/Mercier_PISTACH.pdf

Mintourakis I., and Delikaraoglou D., 2010, Comparison between GPS sea surface heights, MSS models and satellite altimetry data in the Aegean Sea. Implications for local geoid improvement. In: Mertikas S. (ed.), Gravity Geoid and Earth Observation GGEO2008, International Association of Geodesy Symposia, Vol. 135, pp. 67-73

Mintourakis I., 2014, Adjusting altimetric sea surface height observations in coastal regions. Case study in the Greek seas, Journal of Geodetic Science, 4, 109-122, doi: 10.2478/jogs-2014-0012

Mulet S., Rio M. H., and Bruinsma S., 2012, Assessment of the preliminary GOCE geoid models accuracy for estimating the ocean mean dynamic topography, Mar. Geod., 35, 314-336, doi: 10.1080/01490419.2012.718230

Nittis K., Perivoliotis L., Korres G., Tziavos C., and Thanos I., 2006, Operational monitoring and forecasting for marine environmental applications in the Aegean Sea, Environmental Modelling & Software, Volume 21 (2), 243-257, doi: 10.1016/j.envsoft.2004.04.023

Oddo P., Adani M., Pinardi N., Fratianni C., Tonani M. and Pettenuzzo D., 2009, A Nested Atlantic-Mediterranean Sea General Circulation Model for Operational Forecasting, Ocean Sci. Discuss., 6, 1093-1127

Permanent Service for Mean Sea Level (PSMSL), 2018, Tide Gauge Data, Retrieved 20 Jul. 2018 from http://www.psmsl.org/data/obtaining

Pugh, D., and Woodworth, P.L., 2014, Sea-Level Science: Understanding Tides, Surges, Tsunamis and Mean Sea-Level Changes, Cambridge Univ. Press, Cambridge, U. K.

Poulain P.M., Menna M., and Mauri E., 2012, Surface Geostrophic Circulation of the Mediterranean Sea Derived from Drifter and Satellite Altimeter Data, Journal of Physical Oceanography, 42(6), 973-990, doi: 10.1175/JPO-D-11-0159.1

Reigber, C., Casper, R. and Päffgen, W., 1999, The CHAMP Geopotential Mission, IAA 2nd International Symposium on Small Satellites for Earth Observation, Berlin, April 12-16, 1999, pp. 25-28

Rio M.H., Poulain P.M., et al., 2007, A Mean Dynamic Topography of the Mediterranean Sea computed from altimetric data, in-situ measurements and a general circulation model, Journal of Marine Systems vol.65: pp 484-508, doi: 10.1016/j.jmarsys.2005.02.006

Rio M.-H., Pascual A., Poulain P.-M., Menna M., Barceló B., and Tintoré J., 2014a, Computation of a new mean dynamic topography for the Mediterranean Sea from model outputs, altimeter measurements and oceanographic in situ data, Ocean Science, 10, 731-744, doi: 10.5194/os-10-731-2014

Rio M.H., Mulet S., and Picot N., 2014b, Beyond GOCE for the ocean circulation estimate: Synergetic use of altimetry, gravimetry, and in situ data provides new insight into geostrophic and Ekman currents, Geophys. Res. Lett., 41, doi: 10.1002/2014GL061773

Rummel R., 2001, Global unification of height systems and GOCE. In: Sideris M.G. (ed.), Gravity, geoid and geodynamics 2000. Springer, Berlin, pp 13-20. doi:10.1007/978-3-662-04827-6_3

Simoncelli S., Fratianni C., Pinardi N., Grandi A., Drudi M., Oddo P., and Dobricic S., 2014, Mediterranean Sea physical reanalysis (MEDREA 1987-2015) (Version 1) set. E.U. Copernicus Marine Service Information. doi: 10.25423/medsea_reanalysis_phys_006_004

Slobbe1 D.C., Klees R., Verlaan M., Zijl F., Alberts B., and Farahani H.H., 2018, Height system connection between island and mainland using a hydrodynamic model: a case study connecting the DutchWadden islands to the Amsterdam ordnance datum (NAP), Journal of Geodesy, 92, 1439-1456

Soukissian T., Chronis G., and Nittis K., 1999. POSEIDON: Operational marine monitoring system for Greek seas. Sea Technology, 40, 31-37

Tapley, B. D., Bettadpur, S., Watkins, M. and Reigber, C., 2004, The gravity recovery and climate experiment: Mission overview and early results, GEOPHYSICAL RESEARCH LETTERS, VOL. 31, L09607, doi:10.1029/2004GL019920

Woodworth P. L., Hughes C. W., Bingham R. J., and Gruber T., 2012, Towards worldwide height system unification using ocean information. Journal of Geodetic Science, 2(4), 302–318. https://doi.org/10.2478/v10156-012-0004-8

Woodworth P.L., Gravelle M., Marcos M. and Wöppelmann G. and Hughes C.W., 2015, The status of measurement of the Mediterranean mean dynamic topography by geodetic techniques, Journal of Geodesy, 89, 811-827 doi: 10.1007/s00190-015-0817-1

Wöppelmann G., 2004. SONEL. In: actes de l'Atelier Expérimentation et Instrumentation IFREMER, INSU, Météo-France, Paris, 23-24 Mars 2004.

Wunsch C., and Stammer D., 1998, Satellite altimetry, the marine geoid, and the oceanic general circulation. Ann. Rev. Earth Planet Sci., 26, 19-253. doi: 10.1146/annurev.earth.26.1.219

Zijl F., Verlaan M., and Gerritsen H., 2013, Improved water-level forecasting for the northwest European shelf and north sea through direct modelling of tide, surge and non-linear interaction. Ocean Dynamics, 63(7), 823-847, doi: 10.1007/s10236-013-0624-2